Hindawi
Mathematical Problems in Engineering
Volume 2022, Article ID 5753651, 18 pages
https://doi.org/10.1155/2022/5753651

Research Article

Passive Power Filter Optimization Problem Based on Adaptive Multipopulation NSGA-II and CRITIC-TOPSIS

Ye Yuan and Cheng Liu

College of Electrical and Information Engineering, Beihua University, Jilin, China

Correspondence should be addressed to Cheng Liu; liucheng@beihua.edu.cn

Received 19 August 2022; Revised 28 September 2022; Accepted 12 October 2022; Published 25 October 2022

Academic Editor: Yang Li

The best configuration of passive filters in extra-high voltage systems is investigated in this study using a two-stage multiobjective decision-making (MODM) framework. A collection of Pareto solutions is found using an adaptive multipopulation-modified nondominated ranking genetic algorithm (AMP NSGA-II) in the first stage. The goals taken into account include the least fundamental reactive power compensation losses, overall cost and maintenance cost, and simultaneous minimum harmonic current distortion rate. The objective weights are determined and the optimum solution is chosen in the second stage using the criteria importance interrelationship (CRITIC) and similarity ranking preference technique (TOPSIS). A number of examples show how the suggested method performs more effectively than the conventional and well-known algorithm and can identify the relationship between the objective functions, indicating that the suggested scheme has better superiority in filters and has a promising future in the solution of multiobjective problems.

1. Introduction

1.1. Background. In order to meet the urgent demand for clean energy and energy transmission, load center power supply, and energy conservation, the national grid vigorously develops UHVDC (ultrahigh voltage direct current) technology suitable for long-distance and large-capacity transmission. This is due to the unfavorable distribution of energy and user loads in China. The grid's capacity to efficiently allocate resources on a wide scale has greatly increased with the completion of the UHVDC interconnection grid. The grid's integration is also growing in importance, with a closer connection between the transmitter and receiver, AC and DC. The grid operation, in short, offers a lot of novel features [1].

Due to the fact that the current in nonlinear devices is not inversely proportional to the applied voltage, both the current and voltage waveforms are distorted [2]. The ensuing harmonics could cause a variety of power quality issues that need to be addressed. The models of the network components in the power system must be carefully created in order to handle this harmonic problem. Researchers in several studies make the supposition that all loads are linear. Since the majority of the electrical loads in the power system have inhomogeneous rates of electricity consumption, this assumption is typically erroneous [3].

As a result, nonlinear loads are frequently employed to effectively resolve load modeling issues. Both linear and nonlinear loads ought to be accounted for in the load model [4]. Nonlinear loads may also introduce harmonic currents into the power system, causing distortion.

Consumers frequently employ nonlinear loads [5–7] in power systems, which have nonsinusoidal currents and frequently affect communication even when they are coupled to a sinusoidal power source. The waveform may be distorted because of the load's nonlinear behavior. The distortions in the current and voltage waveforms [8–10], which are expressed as harmonics, are caused by the increase in nonlinear loads. These harmonics can have a negative impact on the power system in a variety of ways, including power loss, a drop in power factor, equipment failure, wear and tear, and damage [11–17]. Several methods have been

devised to address these issues, employing elements such as reactors, chokes, active power filters (APF), passive power filters (PPF), alternative transformer connections, and converters with greater pulse counts. Due to their simplicity and low cost, PPFs are the most efficient and widely used method [18].

It is crucial to set up the UHVDC system's PPF-sized planning architecture based on the known load demand and constrained resources. Underconfiguration may have an impact on the system, impacting the regular power supply and electricity usage [19, 20]. Overconfiguration of PPF may result in cost increase and overcompensation, creating avoidable losses. Therefore, in this research, the study configures the PPF sizing plan layout using a two-stage multicriteria decision making (MCDM) framework. The three goals, namely, harmonic current distortion rate, overall cost and maintenance cost, and least fundamental reactive power compensation loss—as well as some of the aforementioned constraints—are used in the first step. The adaptive multipopulation NSGA-II is solved to produce the Pareto front. The weights of the objectives are then determined using the CRITIC and TOPSIS procedures, respectively, and the best choice is then made out of a large number of options.

1.2. Literature Review. The focus has always been on the study and application of passive filters, but distinct papers frequently have varied entrance points, purposes, and approaches. Bagheri Ali and Alizadeh Mohsen construct passive filters in the study [21] for a microgrid that combines nonlinear loads, solar panels, and wind turbines. They chose a sample of harmonic microgrids using the ETAP program to learn more about the layout of passive filters and afterwards alter the parameter values. Gurrola-Corral, in his study [22], introduced a design method based on extended harmonic domain modeling and showed how to use the resulting power quality and steady-state waveforms to identify the passive filter. He also demonstrated how to demonstrate the method's efficacy. In the article [23], Shakeri Sina concentrated on the sensitivity of nonlinear loads (LCI) at PCC voltage sag, combining cost effectiveness, detuning effects, and taking into account harmonic loads of resonant capacitors. She also verified the generality and applicability of the considered approach based on the annual operations derived from simulations. The study [24] proposes a filter inductance ratio that minimizes the total inductance to determine the three filtering elements of the LCL filter (inverter-side inductance, grid-side inductance, and filter capacitor) and reduces engineering iterative trial and error. Passive filters, as an important component of LCL filters, also play a crucial role in grid-connected inverters in energy storage systems (ESS) or renewable energy systems (RES), and passive filters play an important role. The article [25] suggests a passive filter (PPF)-based cost consideration technique using just one set of PPFs, which not only reduces the amount of space needed to prevent PPFs but also resolves the quality compensation problem of two parallel compensated generators (EGs) and validates their performance using MATLAB. The ideal dual-tuned filter formulation was established in the literature [26] based on the maximum impedance filter characteristic location and the alternative impedance harmonic reduction analysis maximization of the main power supply. Klempka Ryszard took into account the equivalent impedance of the main filter and the detuning of the filter when designing the PPF. Literature [27] presents a modulation-based method for the optimization and unification of grid-connected inverters that finds the maximum ripple current, calculates the precise optimal passive damping resistance, takes into account the design parameters that influence the factors, and uses this algorithm to determine the optimal size of the inductor and capacitor, as well as demonstrates the method's superiority based on damping loss.

More researchers are using algorithms to examine the best PPF design because parts of the processes are not open to the public. In the article [28], Yang Nien-Che proposed the multiobjective bee colony optimization (MOBSO), which employs the Pareto optimality to carry out the best PPF design. The least Manhattan distance strategy is used to choose the most equilibrium solution in the Pareto set among the obtained nondominated solutions. Additionally, Yang Nien-Che invents once more in the publication [29] by revalidating the Pareto solution set based on the artificial bee colony (ABC) method that has been enhanced by applying the artificial intelligence algorithm, which is more effective than the previous one. Khajouei Javad designed the most cost-effective and efficient way to deal with harmonics with passive filters for IEEE networks with nonlinear loads and Steinmetz circuits in the literature [30]. He discussed total harmonic distortion, voltage deviation values, total filter cost, the corresponding frequency, and critical bus power factor in the network and proposed the NSGA-II algorithm to deal with harmonics. The multiobjective optimization problem is proposed to be solved using the NSGA-II algorithm, and finally, the best solution is obtained from the Pareto front using the normalizing approach. Bajaj Mohit contributed to the literature [31] by taking into account constraints such as line current, individual total harmonic distortion (THD) on the common coupling point (PCC) voltage, capacity of the distribution line under overload, and steady-state voltage profile load power factor (PF). He also proposed the Pareto-based multiobjective firefly (pb-MOFA) and entangled three system, namely, performance parameters, (PI)-convergence degree (CM), and generation distance. The MRFO algorithm, which embodies excellent solution-seeking capability but relatively high computational effort, was used in literature [32] to solve the PPF parameter design problem. The resulting PPF can effectively attenuate higher-order harmonics and improve the harmonic performance of the system under various operating conditions. A new fuzzy algorithm based on the nonhomogeneous cuckoo search algorithm (NoCuSa) was proposed in the literature [33] to deal with critical harmonics and power factor improvement problems, specifically by including a resonance index in the problem description, choosing the location of the analyzed passive filter based on sensitivity analysis, and optimizing the filter according to its

value and tuning order under different loads. Literature [34] uses teaching-based optimization (TLBO) with the Pareto optimality that blends fuzzy decision making with external profiles. To increase the variety of nondominated solutions, a teacher selection technique and a group search strategy are employed (NDS). According to literature [35], a Crow's spiral-based exploration approach (CSSA) is suggested for the mathematical design of a new fourth-order harmonic passive filter when minimizing the total demand distortion of the supply current is the only objective. This approach relies on a spiral search mechanism to balance the imbalance of the original algorithm. A Pareto-based multiobjective bat algorithm (pb-MOBA) is suggested in the literature [36] to deal with the minimum total filter cost (FC) and the distortional grid harmonic constrained carrying capacity (HC) of the optimal distributed generation (DG) system for renewable energy sources, to obtain the Pareto optimal front and discuss the trade-offs between the study objectives.

The NSGA-II algorithm is developing and attracting a growing amount of scholarly interest. The effectiveness of NSGA-II has been tested using a variety of multiobjective test problems and it has been found that by slightly altering the algorithm's objective values, the antidominance solution's negative effects can be offset. Arshad M.H. employed NSGA-II and TOPSIS decision making for the conventional model in the literature [37]. The nonlinearity of the induction motor (IM) intrinsic model was shown to be significantly better managed using predictive control (MPC) optimization. The initialization and evolution of the backward learning mechanism, as well as the dynamic adjustment of the crossover probability and the variation probability in accordance with the exponential distribution, were all mentioned by Xiaoqing Li in literature [38]. The enhanced NSGA-II was used to implement variable pitch and variable torque control at their best. The findings collected demonstrate how well this revised algorithm controls front-end speed regulation (FESR) wind turbine power. The NSGA-II algorithm framework and local simulated annealing (SA) are combined in literature [39], with the former used to take into account the objective problem and evaluate each bicriteria individual and the latter used to account for the uncertainty of the scenario description. The resulting hybrid algorithm produces a significantly better set of Pareto solutions for the bicriteria problem than the other cases. The distributed generating units (DG) in series with the fault current limiter (FCL) optimization problem is addressed by Hamidi Mir Emad in literature [40]. He proposed to study this problem using the NSGA-II algorithm with the goal of determining the best location and size for the DG and the best size for the FCL. The method was then implemented in power networks and the effectiveness of the approach was demonstrated. Literature [41] also makes use of the Pareto-based MOO technique, which produces more effective outcomes when dealing with unique categorization challenges. A new adaptive multiobjective adaptive intelligent search and optimization algorithm based on the Gray Wolf optimizer is proposed by Yildirim Gungor in literature [42] when dealing with multiobjective optimization problems. This algorithm is better able to handle situations where there are not enough data sets and increases the effectiveness of getting results. In order to improve the performance of the algorithm, Xu Fangqiu in the literature [43] substituted the orthogonal array and the Taguchi method for the NSGA-II crossover operation. By choosing the neighbors with the greatest distance from one another for the crossover operation, Yijie Sun also enhanced the conventional NSGA-II crossover operation in the literature [44], which enhanced the convergence of the population distribution by utilizing hybridization.

Multiattribute decision making (MADM) is used to determine the best answer when utilizing multiobjective evolutionary algorithms, which frequently yield a number of Pareto solutions and make it challenging for the decision maker to choose the best one. According to literature [45], the Pareto front on the optimization problem of geometric parameters in an inducer installed upstream of a centrifugal pump's inlet was derived using a modified NSGA-II. The Pareto front was then combined with a preference ranking technique of ideal solution similarity (TOPSIS) to determine the ideal point of equilibrium. In the literature, Yang Wei [46] stated that he suggested a linear programming model to calculate attribute weights based on similarity function and the Lagrangian function for ranking using TOPSIS approach and studied the application of the method in the face of known partial attribute weights. In addition to the initial integrated multicriteria decision making (MCDM)-TOPSIS simulation technique, Samala Thirupathi advocated employing the entropy method to estimate the weights of each parameter. The method's validity has been demonstrated in literature [47] for both typical and atypical operating circumstances. According to literature [48], NSGA-II and the VIKOR method are combined to create the Pareto front, from which the best solution is then chosen. In literature [49], an economic and technological trade-off was discovered using multiobjective particle swarm optimization (MOPSO) and the optimal solution was discovered using the weighted sum approach.

The study [50] presents a two-step approach to optimizing reactive power dispatch based on the IEEE30 bus and the IEEE118 bus. The article uses multiobjective optimization (MOO) and Pareto-dominated multiobjective evolutionary algorithm (CPMOEA) in the application of the fuzzy C-mean algorithm (FCM), cleverly combined with the grey correlation projection method (GRP). The decision-making process takes full account of the decision maker's preferences and provides a good solution for the decision maker, besides presenting specific problems and application prospects for future work. In the study [51], in the first step, the dominant evolutionary algorithm (DEA) is used to find the Pareto optimal solution. In the second step, FCM and GRP are used to find the compromise solution, which also shows the focus's limitations and future possibilities.

In this study, the ideal passive filter configuration for the UHVDC system is taken into account using a two-stage decision-making framework. First, Pareto solutions are obtained using adaptive multipopulation NSGA-II while taking into account the goals of the minimum harmonic distortion rate, total cost and maintenance cost, and the

minimum basic reactive power compensation losses. The weights of these three goals are then calculated using CRITIC and TOPSIS, and the one optimal option is then chosen from the numerous Pareto solutions. The Yunguang UHVDC system's passive filter setup is handled using the proposed framework. Decision makers may find this study useful in developing better optimization algorithms and decision frameworks.

1.3. Research Specific Contributions. The specific contributions of this study are as follows: (i) The first introduction of the adaptive multipopulation NSGA-II to the optimal configuration of passive filters. (ii) The simultaneous consideration of the objectives of minimum harmonic distortion rate, overall cost and maintenance, and minimum fundamental reactive power compensation loss. (iii) The first use of two-stage decision making to consider the optimal configuration of passive filters for UHVDC systems. (iv) Applied to real engineering data to solve real engineering problems. (v) Used data results to demonstrate the effectiveness of the decision framework.

1.4. Paper Organization. The remaining portions of this study are structured as follows: The PPF design is discussed in Section 2 after this section, and the two-stage framework is presented in Section 3 together with the objective constraints and optimization technique. An explanation of the required framework and to-be-used algorithms are provided in Section 4. The case study and validation of the suggested framework are presented in Section 5. The conclusions are presented in the last section.

2. Classification and Characteristics of Passive Power Filters

2.1. Passive Power Filter Types. Passive, active, and hybrid filters are all used in power filters. All of these can be efficient at removing harmonics, but in the industrial setting, passive filters frequently have straightforward configurations due to their low price. Passive filters are usually divided into four categories, depending on how the capacitors, resistors, and inductors are paired. These types are listed in Figure 1. Figure 1(a) shows monotonic filters (ST), Figure 1(b) shows second-order damped filters (SD), Figure 1(c) shows C-type damped filters (CD), and Figure 1(d) shows third-order damped filters (TD). The harmonic impedance of each type of passive filter is presented in Table 1.

2.2. System Harmonic Model Characteristics. PPF is a popular option for UHVDC systems to improve power quality because it is both cost-effective and effective at reducing harmonics. The described system, which includes a power supply, transformer, passive filter, and nonlinear load, can be seen in Figure 2(a). To filter and account for harmonic currents and reactive power, the system typically employs a set of monotonic C-type filters, reactive power compensation capacitor elements, and a set of second-order high-pass filters. The relationship between system current and voltage is depicted in Figure 2(b).

3. Two-Stage MCDM Framework

In this study, it is pointed out that the passive filter optimization problem in UHVDC systems can be divided into two stages of MCDM, which is a multicriteria decision making (MODM), considering the objectives of simultaneous minimum harmonic current distortion rate, overall cost and maintenance cost, and minimum fundamental reactive power loss. A set of Pareto solutions are obtained by adaptive multipopulation modified nondominated ranking (NSGA-II), while the second stage is the multiattribute decision making (MADM), which uses criteria importance interrelationship (CRITIC) and similarity ranking preference technique (TOPSIS) to determine the objective weights and select the single best solution. Figure 3 shows a depiction of the MCDM framework.

3.1. Objective Functions. In order to meet the demands of harmonic filtering and power factor improvement, the design of the PPF depends on choosing the proper filter type and optimizing the parameters of the components (R, L, and C). To create the filter at the lowest possible investment cost, it is also necessary to take the investment cost of the PPF design into account. Naturally, to achieve this, a few objective functions and a few constraint optimization model functions must be satisfied. The aim and constraint functions' makeup is given below.

3.1.1. Minimum Current Harmonic Distortion Rate. The minimum harmonic distortion rate can be used to gauge how well the harmonizer is working. The filter's performance is acknowledged if it is able to successfully filter the system's harmonics so that the harmonic content complies with national criteria. The IEEE519 necessary harmonic content is employed as a reference value with the following objective function, and the minimal harmonic distortion rate of the system is used as a satisfaction criterion in this research:

$$\min THDI = \sqrt{\sum_{h=2}^{N} \left(\frac{I_{sh}}{I_1}\right)^2}. \quad (1)$$

Here, h stands for harmonics and N stands for the highest harmonic number, where I_1 is the root mean square of the fundamental current.

3.1.2. Overall Cost and Maintenance Costs. The overall cost and maintenance cost as an economic indicator include the total cost of filtering various devices and the maintenance cost. The main costs of the filter include the cost

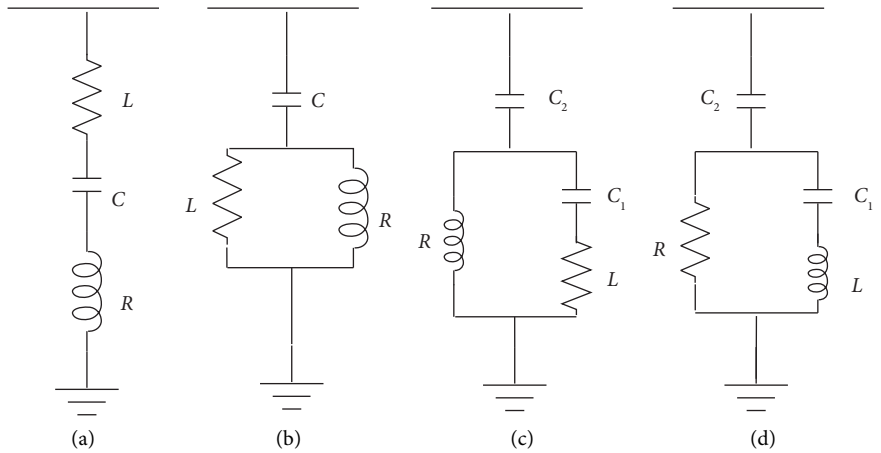

Figure 1: Classification of passive filters, namely, (a) monotonic filters, (b) second-order damping filters, (c) C-type damping filters, and (d) third-order damping filters.

Table 1: The harmonic impedance of each type of a passive filter.

Type	$R_F(h)$	$X_F(h)$
ST	R	$hX_L - X_C/h$
SD	$R(hX_L)^2/R^2 + (hX_L)^2$	$R^2hX_L/R^2 + (hX_L)^2 - X_C/h$
CD[1]	$R(hX_L - X_L/h)^2/R^2 + (hX_L - X_L/h)^2$	$R^2(hX_L - X_L/h)/R^2 + (hX_L - X_L/h)^2 - X_C/h$
TD[2]	$R(hX_L)^2/R^2 + (hX_L - X_C/h)^2$	$R^2hX_L - hX_L^2X_C + X_LX_C^2/h/R^2 + (hX_L - X_C/h)^2 - X_C/h$

[1]In CD PPFs, $X_C = 1/(\omega C_2), C_1 = 1/(\omega_1^2 L)$,[2]In TD PPFs.$X_C = 1/(\omega C_2), C_1 = C_2$

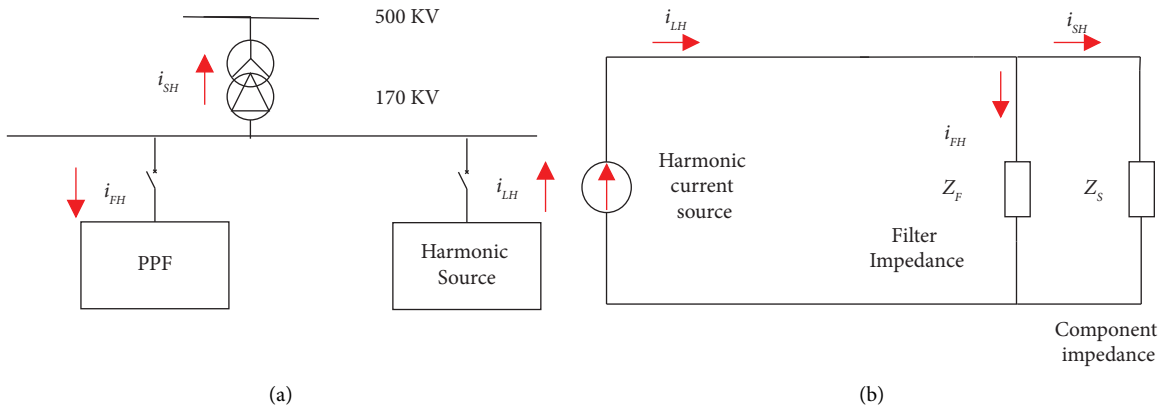

Figure 2: Simple harmonic circuit with nonlinear load and PPF. (a) Single line diagram. (b) Equivalent harmonic model.

and maintenance of inductors, reactors, and capacitors. Therefore, the economical objective function is as follows:

$$\min F = \sum_{i=5,7,11,13} (k_1C_i + k_2L_i + k_3R_i). \quad (2)$$

The functional expression in this case is an innovative way of assigning the cost of capacitors, inductors, and reactors based on the specific number of filtered harmonics, rather than the type of PPFs, with i representing the number of filtered harmonics responsible in a given high-voltage system, where noncharacteristic harmonics account for almost all and special diagnostic harmonics are negligible.

3.1.3. Minimum Basic Reactive Power Compensation Loss. After the system is installed with PPF, the power factor of the system should be maintained at a level close to unity, and there should not be too much compensation or too much undercompensation, which are losses of reactive power compensation for the system. Undercompensation cannot be allowed in the actual working conditions. The capacitor

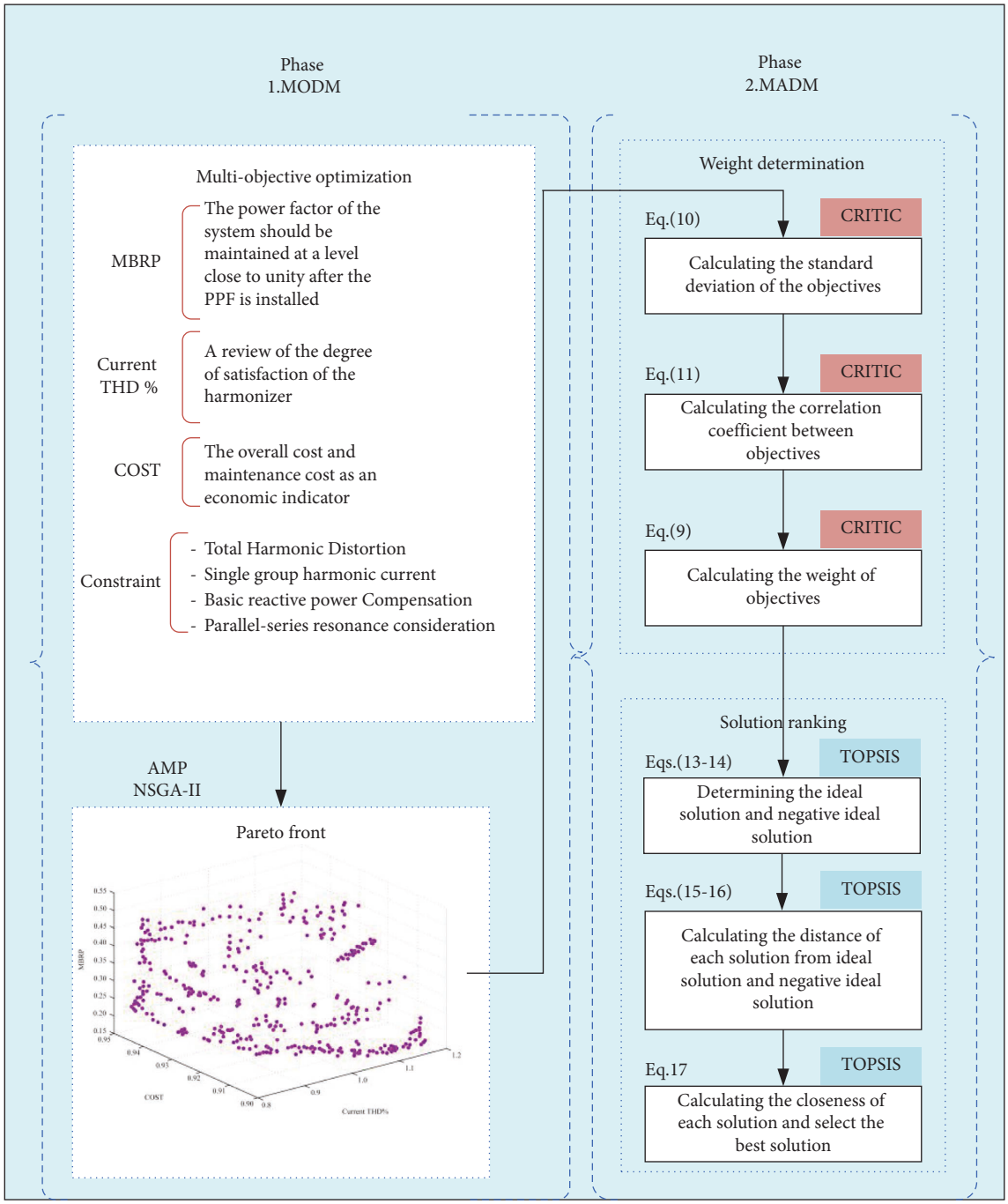

Figure 3: A depiction of the MCDM framework.

provides the main reactive power, i.e., the minimum basic reactive power compensation loss function is as follows:

$$\min \sum_{i=5,7,11,13} Q_{ci-loss}. \tag{3}$$

3.2. Constraints. In order to guarantee that the resultant solution set is finite, the NSGA-II multiobjective evolutionary optimization algorithm additionally needs parametric constraints that set a range of values after the parametric optimization function. The permitted harmonic levels are dependent on the national specification because the IEEE standard enables higher allowable harmonic levels than the national standard.

3.2.1. Total Harmonic Distortion. The overall harmonic filter needs to meet the criteria that after compensation the THD must meet the following:

$$THDI \leq THDI_{MAX}. \tag{4}$$

3.2.2. Single Set of Harmonic Currents. For the harmonic filtering requirements of a single group PPF, each harmonic should satisfy the criterion, where h represents the $12k\pm1^{st}$ harmonic and $I_{h\max}$ is the maximum permissible level of h-th order harmonic current. Constraints include the following:

$$I_{sh} \le I_{h\max}. \tag{5}$$

3.2.3. Basic Reactive Power Compensation. The compensation for basic reactive power must be constrained, where Q represents the lowest and upper bounds of the total basic reactive power, respectively. The constraint functions are as follows:

$$Q_{\min} \le \sum_{i=5,7,11,13} Q_i \le Q_{\max}. \tag{6}$$

3.2.4. Parallel-Series Resonance Limit Consideration. Parallel and series resonance limits are as follows: when analyzing the PPF, the system source resonance limit must be considered, although according to literature [49], it is known that the harmonic impact of this generated by this UHVDC system can be negligible law; therefore, it is not set as a constraint function.

4. Optimization Algorithm

4.1. Conventional NSGA-II. NSGA-II is an enhanced version of the original NSGA with the addition of a nondominated sorting method for both the rank level and crowding distance components of Pareto sorting. Individuals with a lower rank are preferred, whereas those with a larger crowding distance (i.e., a lower estimated density) are chosen for the same rank level. In comparison to NSGA, literature [52] demonstrates that NSGA-II eliminates the complex fitness sharing strategy that requires specifying the sharing radius. The introduction of the elite retention strategy ensures the retention of the best individuals and the distribution of solution sets. It is successfully used in a wide variety of industries, indicating that it is more valuable for use in a wide variety of multiobjective optimization algorithms.

The steps of the conventional NSGA-II algorithm are as follows, where the flowchart can be seen in Figure 4:

(1) First, begin by populating the population. Then, we generate an initial population of size N_p at random.

(2) Fast nondominated sorting is done. For each individual in the population, the Pareto rank is compared to obtain its dominated number $n_p = 0$. All individuals on F_1 are removed, and the preceding procedure is repeated for the remainder of the population in order to complete the population's hierarchy.

(3) Crowding degree calculation is done. The individuals in the same nondominated layer are sorted according to the size of the objective f_m. The crowding degree n_d of the two boundary solutions after sorting is infinity, and the crowding degree of the remaining individuals is as follows:

$$n_d = n_d + \frac{\left[f_m(i+1) - f_m(i-1)\right]}{\left(f_m^{\max} - f_m^{\min}\right)}. \tag{7}$$

(4) Bid-race selection is done. Binary bidding tournament selection was used to randomly select 2 individuals, and the individual with Pareto rank engaged was selected to enter the next generation population, and the individual with the same rank was selected to crowd the larger one.

(5) Variational crossover variants, using simulated binary crossover and polynomial variants are considered.

(6) A new population is generated. Using the elite retention strategy, the parent population P_i and the offspring population C_i are mixed to form a new population R_i. The new population R_i is sorted nondominantly, and the dominant pole $F_1, F_2, \cdots, F_m$ is placed into the new parent population P_{t+1} in descending order of Pareto rank until the size of P_{t+1} exceeds that of N_p. The individuals in P_{t+1} are removed from F_m in descending order of crowding until the size of P_{t+1} equals that of N_p.

4.2. Adaptive Multipopulation NSGA-II. In the traditional NSGA-II, when solving a multiobjective optimization problem, the initial population is subjected to nondominated sorting and crowding degree calculation and then to selection, crossover, and variable pressure, merging the child population with the parent population and nondominated sorting to obtain a set of Pareto solution sets which are theoretically optimal. However, there is poor diversity and the populations converge centrally at local optima.

In the adaptive multipopulation nondominated sorting genetic algorithm (adaptive multi-population NSGA-II, AMP NSGA-II) studied in this study, we use the indirect equilibrium idea to establish the genetic operation of multiple populations and multiple crossover operators and we use the logistic model to make reasonable adaptation to the crossover operator assignment in the population.

The flowchart is shown in Figure 5. The following is a specific description of the AMP NSGA-II process.

(7) A population is divided into several subpopulations and given distinct crossover operators first. According to literature [49], it is known that parent-centered crossover (PCX) and mixed crossover (BLX-α), when combined, are suitable for solving individual class multiobjective problems. When used individually, simulated binary crossover (SBX), simple crossover (SPX), and mixed crossover (BLX), when used individually, are also suitable. According to various operators, different optimization techniques are allocated to the four

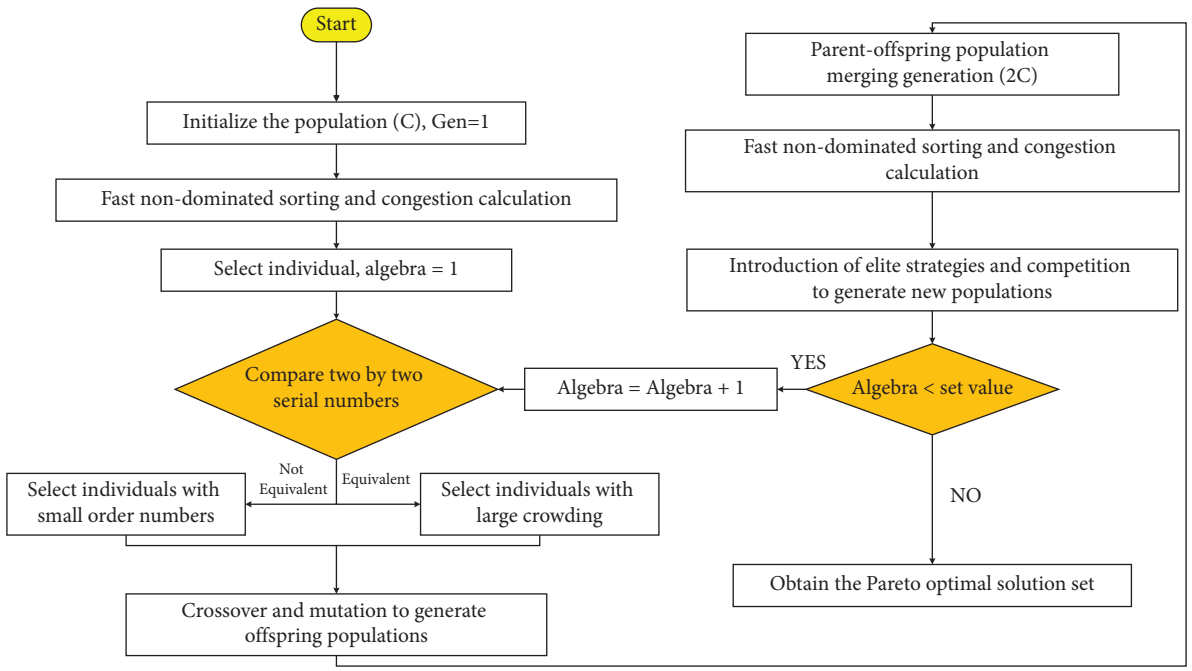

Figure 4: NSGA-II algorithm flowchart.

subpopulations. Additionally, because different crossover operators will have different global search capabilities and search strategies to create diverse populations, the distribution of individuals will be improved, the genetic algorithm will function more efficiently, and the outcomes will be more convergent. The original NSGA-II mutation operator is still present in AMP-NSGA-II, making it simple to change the values of select genes on specific chromosomes and avoid the "premature" issue.

(8) Next, the four subpopulations that are finished dividing are selected by binary race and mutated to produce new populations. The parent population is merged with the subpopulations for noninferiority ranking and crowding ranking to obtain the superior individuals, which are then incorporated into the EXS solution set.

(9) The integration of the best individuals into the EXS set makes the constant approach to the Pareto optimal solution set. The best individuals are also in constant competition, in three cases, as follows:

(i) If the individual solution is better than the solution in the EXS solution set, the EXS solution set removes the eliminated solution and adds the better solution.

(ii) If an individual solution is not as good as the worst solution in the EXS solution set, it is not processed and invalidated.

(iii) If the EXS solution set exceeds the set value NEXS, the solutions in the EXS solution set will be sorted for noninferiority and congestion, and the poor solutions will be removed.

(10) The contribution of the populations of the four allocated finished various variational operators will be used to create the EXS solution set, while the overall number of people and the size of each population will remain constant. By adjusting the size of each population to achieve the desired subpopulation for various adaptive optimization problems, the goal is to increase the density of individuals on the Pareto front and decrease the number of populations with a lower density on the Pareto front. Additionally, the goal is to quickly find the best set of solutions for various multiobjective optimization problems in order to significantly increase population adaptability. This is the so-called logistic model. The specific steps of the logistic model are listed in Figure 6.

4.3. CRITIC-TOPSIS. The objective weighting approach is crucial in this study since it is challenging for the decision maker to provide a meaningful subjective assessment of the three objectives. As seen above, the adaptive multigroup NSGA-II algorithm produces the Pareto front from the collection of EXS solutions, and the CRITIC-TOPSIS decision aids in both selecting the unique optimal solution and extracting the objective weights from the Pareto front. The combination of a similarity function and a Lagrangian function is mentioned in literature [46] as a strategy to find the best answer. On the other hand, literature [47, 52] apply the weighting approach and the entropy method, respectively. It must be realized that there are minor inconsistencies between the three PPF optimization objectives while considering them in this study. The minimum harmonic

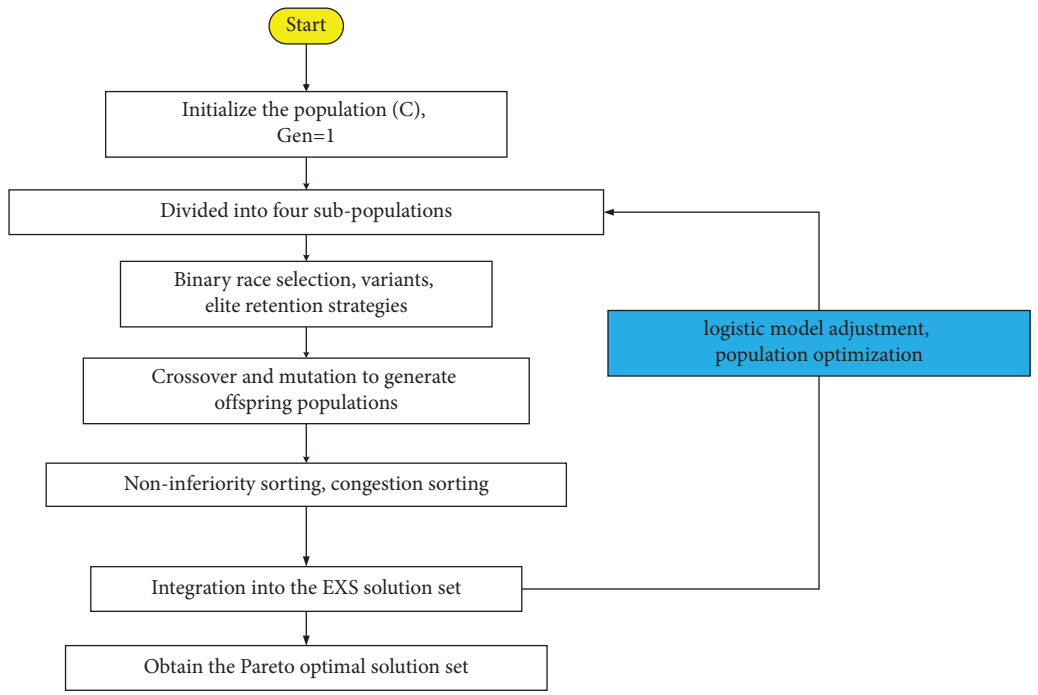

Figure 5: AMP NSGA-II algorithm flowchart.

1	The estimated contribution of $P_{i,t+1}$ (i=1,2,3,4) to the update of EXS solution is c_i;
2	Determine the population that contributes most to the EXS j : $\{j \backslash c_i = \max_{i-1,2,3,4} \{c_i\}\}$;
3	Calculate the crossover operator for EXS-self-Update operation Crossoveroperator (j);
4	If $j \leq 2$;
5	For k : = 1 to $\{N_{EXS} / 2\}$;
6	Two crossover individuals p_1 and p_2 are randomly selected from the EXS solution set;
7	For individuals p_1 and p_2, crossover operations are performed with Crossoveroperator (j) Crossover operators to generate offspring individuals q_1 and q_2;
8	Update the EXS solution set with individuals q_1 and q_2;
9	End for
10	End if
11	If $j \geq 3$;
12	For k : = 1 to $(N_{EXS} / 3)$;
13	Three crossover individuals , p_1 , p_2 and p_3 are randomly selected from the EXS solution set
14	For individuals p_1, p_2 and p_3, crossover operations are performed with Crossoveroperator (j) crossover operators to generate off spring individuals q_1, q_2 and q_3;
15	Update the EXS solution set with individuals q_1, q_2 and q_3;
16	End for
17	End if

Figure 6: Logistic model.

distortion rate and basic reactive power compensation will both be impacted by pursuing lower cost spending, and vice versa. Pursuing the minimum harmonic distortion rate will increase overall cost and maintenance as well as lead to overcompensation, which makes the increased reactive power compensation into consideration. The entropy approach and the weighting method cannot be used due to the conflicts between these three goals.

For resolving conflicts between objectives and weighing the weights of the objectives, we use Diakoulaki Mavrotas' CRITIC approach from literature [53]. The CRITIC technique represents the conflicts between objectives using correlation coefficients. The following is the normalized decision matrix A_{ij} with the number of Pareto schemes set to m, the number of objectives set to n, and the standard deviation used to weigh the dispersions in the schemes as follows:

$$A_{ij} = \begin{bmatrix} a_{11} & a_{12} & \cdots & a_{1n} \\ a_{21} & a_{22} & \cdots & a_{2n} \\ \vdots & \vdots & \vdots & \vdots \\ a_{m1} & a_{m2} & \cdots & a_{mn} \end{bmatrix}, \tag{8}$$

$$w_j = \frac{\sigma_j \sum_{i=1}^{n}\left(1 - r_{ij}\right)}{\sum_{j=1}^{m}\left(\sigma_j \sum_{i=1}^{n}\left(1 - r_{ij}\right)\right)}, \tag{9}$$

$$\sigma_j = \sqrt{\sum_{i=1}^{m} \frac{\left(a_{ij} - \bar{a}_j\right)^2}{m-1}}, \tag{10}$$

$$r_{ij} = \frac{\sum_{x=1}^{m}\left(a_{ix} - \bar{a}_i\right)\left(a_{jx} - \bar{a}_j\right)}{\sqrt{\sum_{x=1}^{m}\left(a_{ix} - \bar{a}_i\right)^2}\sqrt{\sum_{x=1}^{m}\left(a_{jx} - \bar{a}_j\right)^2}}. \tag{11}$$

Here, w_j, σ_j, and r_{ij} represent the target weights, standard deviations, and correlation coefficients, respectively. Combining the normalized matrix with the objectives, the matrix is as follows:

$$\begin{aligned} V_{ij} &= \begin{bmatrix} v_{11} & v_{12} & \cdots & v_{1n} \\ v_{21} & v_{22} & \cdots & v_{2n} \\ \vdots & \vdots & \vdots & \vdots \\ v_{m1} & v_{m2} & \cdots & v_{mn} \end{bmatrix} \\ &= \begin{bmatrix} a_{11} \cdot w_1 & a_{12} \cdot w_2 & \cdots & a_{1n} \cdot w_n \\ a_{21} \cdot w_1 & a_{22} \cdot w_2 & \cdots & a_{2n} \cdot w_n \\ \vdots & \vdots & \vdots & \vdots \\ a_{m1} \cdot w_1 & a_{m2} \cdot w_2 & \cdots & a_{mn} \cdot w_n \end{bmatrix}. \end{aligned} \tag{12}$$

TOPSIS is often used to solve multiobjective and multiattribute decision making problems (MADM). Literature 46 uses TOPSIS decision making to find the equilibrium optimum, literature 47 uses TOPSIS ranking, and literature 48 uses the VIKOR technique to find the optimal solution. The TOPSIS method is a comparative understanding method. The TOPSIS is fully known as the similarity ranking preference technique, and its core idea is similar to the above NSGA-II congestion ranking. The idea is actually to list the solutions to be used for comparison between the optimal solution and the worst solution and derive a good or bad pair of solutions based on calculating the distance between the solutions as follows:

(11) First, the ideal optimal solution z_j^+ and the ideal worst solution z_j^- of the objectives are determined. F_1 and F_2 represent the set of benefit objectives and the set of cost objectives, respectively, as follows:

$$\begin{aligned} z_j^+ &= \begin{cases} \max_{1 \leqslant i \leqslant m}\left(v_{ij}\right), & \text{if } f_j \in F_1, \\ \min_{1 \leqslant i \leqslant m}\left(v_{ij}\right), & \text{if } f_j \in F_2, \end{cases} \\ z_j^- &= \begin{cases} \max_{1 \leqslant i \leqslant m}\left(v_{ij}\right), & \text{if } f_j \in F_1, \\ \min_{1 \leqslant i \leqslant m}\left(v_{ij}\right), & \text{if } f_j \in F_2. \end{cases} \end{aligned} \tag{13}$$

(12) The following formula is used to determine how far the solution is from both the ideal optimal solution and the ideal worst solution:

$$\begin{aligned} S_i^+ &= \sum_{j=1}^{n}\left(v_{ij} - z_j^+\right)^2 i = 1, 2, \cdots, m, \\ S_i^- &= \sum_{j=1}^{n}\left(v_{ij} - z_j^-\right)^2 i = 1, 2, \cdots, m. \end{aligned} \tag{14}$$

(13) According to the distance solution, the solution's proximity to the ideal optimal solution is assessed. There are two ways to compare these two options; one says that the answer is better if it is closest to the ideal optimal solution, and the other says that the solution is better if it is farthest from the ideal worst solution. The comparison with the worst-case scenario is used in this instance as follows:

$$C_i = \frac{S_i^-}{S_i^+ + S_i^-} i = 1, 2, \cdots, m. \tag{15}$$

There are a number of well-known MCDM methods, including AHP (analytical network process), ANP (analytical hierarchy process), TOPSIS, and VIseKriterijumska Optimizacija I Kompromisno Resenje (VIKOR). All these methods undoubtedly help decision makers to make their choices, but how do we choose these methods and do they lead to different results?. In literature [54], it is mentioned that different methods are applied to different problem-solving contexts and that the results obtained will vary, but not too much. It is like buying something, some only support cash or credit card payment, but some can do both, but it is more cost-effective to pay by credit card. These methods are like tools for us to use. AHP is a combination of qualitative and quantitative and hierarchical and quantitative processes of decision making that requires the establishment of a

systematic hierarchical conclusion. The whole process of comparative judgement and calculation is cruder and requires the establishment of a hierarchical model based on human factors. ANP is the same reason that requires the establishment of a network topology artificially. ANP can be used in more complex situations. VIKOR is mainly used to deal with energy consumption and the feasibility of renewable energy sources. VIKOR uses linear normalization and is an eclectic ranking algorithm that allows the decision maker to do something with the alternatives as they see fit. It is more sophisticated than TOPSIS in many respects and can eliminate a lot of the complexity of dealing with less complex mathematical engineering problems and get the ranking results very quickly. However, compared with TOPSIS, VIKOR has certain shortcomings in the evaluation of the performance of the problem. It is difficult to quantify a simple and clear value, making it difficult for decision makers to distinguish. The advantages of TOPSIS are clear, that is, it is simple to program, it does not take into account the number of attributes, and the steps remain essentially the same. The uncertainty of the weights is ignored in the TOPSIS method, making it necessary to use another method to compensate for this shortcoming. The amount of information assigned to the object of evaluation is based on the contrast intensity and conflict. Therefore, the CRITIC-TOPSIS pairing fits well with the research topic of the study.

5. Case Study

In the system at 50 Hz and 170 kV, the filter optimization simulation experiments are conducted to prove the accuracy and superiority of the proposed algorithm. There are many cases of harmonic sources generated in the system as follows: constant DC current contains ripple, phase change voltage is nonstandard sinusoidal, and the converter parameters have slight differences. As in Figure 7, the abovementioned cases are collectively referred to as harmonic sources, and due to the large impedance, ignoring the linear load, the PPF is considered the equivalent impedance. The system generally uses a set of monotonic C-type filters, reactive power compensation capacitor elements, and a set of second-order high-pass filters to filter and compensate for harmonic currents and reactive power. The monotonic C-type filter is used to filter the harmonics of the fifth, seventh, and thirteenth orders, while the second-order high-pass filter is mainly used to filter the harmonics of the eleventh order. Consider the planning of 3 types of harmonic filters. In the case where the system is balanced, the measured percentage of the three without filters, national standards, and IEEE Standard 519–2014 are listed in Table 2. According to Table 2, it can be seen that in Case 1, the 11th harmonic, 13th harmonic ratio, and current THD% have exceeded the national standard and IEEE standard; in Case 2, the 7th, 11th harmonic, and current THD% also exceed the national standard and IEEE standard. In addition, the 11th harmonic ratio and current THD% in Case 3 also exceed the national standard as well as the IEEE standard.

To summarize, the number of filters required is 2. The design cost and maintenance cost of the passive filter are calculated with the original investment and maintenance cost as the standard value. The platform simulation is based on a PC with 16 GB of RAM. The population size N and number of iterations Gen are 500 and 200, respectively, the inertia factor ω is set to 0.6124, the learning factor $c_1 = c_2 = c_3 = 1.62$, the subpopulation contribution threshold α, and the subpopulation diversity contribution threshold β are set to 0.4 and 0.32, respectively. The population contribution λ and diversity thresholds θ were set at 0.02 and 0.13. The specific parameter settings are listed in Table 3.

Figure 8 shows the minimum harmonic current distortion rate (current THD%) and the overall cost. Current THD% ranges from 0.8 to 1.1, COST from 0.90 to 0.96, and MBRP from 0.15 to 0.35. When looking at the relationship between the two, one can see the conflicting contradictions described above, Figure 9(a) shows MBRP versus Current THD%. It is easy to see that MBRP increases as THD% decreases, fulfilling the abovementioned statements that when THD% reduction operation is performed, the reactive power compensation losses will increase in response to this. Figure 9(b) shows the two-dimensional Pareto solution of MBRP versus COST. When COST increases, MRTP decreases as well. In the actual project, the overall cost of construction and maintenance is increased and the desired result is definitely better. Figure 9(c) shows that when considering the Pareto front solution set of Current THD% versus COST, the current distortion rate decreases with higher overall cost and maintenance.

These three diagrams represent the three objective functions, the correlation between two and two, and the conflict and contradiction specifically for the existence, and in line with the objective reality, the functionality of AMP NSGA-II in the MCDM framework is verified.

To verify the superiority of AMP NSGA-II in the MCDM framework, the Pareto scheme solution set is put together with the traditional NSGA-II for comparison. Figure 10 shows that both schemes are almost on the same surface, proving the reasonableness and correctness of the algorithm. The solution set of traditional NSGA-II can be seen to be too dense, showing the drawback of poor diversity, while the solutions in the solution set of AMP NSGA-II are almost uniformly distributed.

The superiority of the algorithm needs to be measured by a metric. GD (general distance) is used to measure whether the updated EXS solution set converges to the true Pareto optimal solution set. GD indicates the distance between the obtained EXS solution set and the true Pareto optimal solution set, and the smaller its value, the more the optimal solution set converges to the true Pareto optimal solution set. It can be calculated by (16).

$$GD = \sqrt{\sum_{i=1}^{|EXS|} \frac{d_i^2}{|EXS|}}. \tag{16}$$

The absolute value EXS is the number of individuals in the EXS population; d_i is the Euclidean distance between individuals $i \in$ EXS and the nearest individual in P$*$ in the target space.

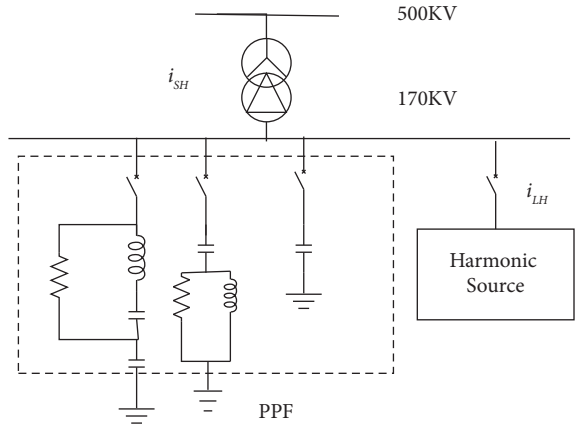

Figure 7: System structure diagram.

Table 2: Case studies without a filter.

Case	Number of harmonics	Measured ratio	National standard	IEEE standard 519–2014
Case 1	5	0.147329	2.61	4
	7	0.131478	1.96	4
	11	4.1524	1.21	2
	13	3.04327	1.03	2
	THD%	5.19563	0.78	5
Case 2	5	0.18423	2.61	4
	7	1.97821	1.96	4
	11	4.1782	1.21	2
	13	1.0237	1.03	2
	THD%	5.68427	0.78	5
Case 3	5	0.56278	2.61	4
	7	1.68743	1.96	4
	11	3.8624	1.21	2
	13	1.0127	1.03	2
	THD%	5.5674	0.78	5

Table 3: Parameter setting.

Parameters	Meaning	Values
N	Population size	500
Gen	Number of iterations	200
ω	Inertia factor	0.6124
c_1, c_2, c_3	Learning factor	1.62
α	Subpopulation contribution threshold	0.4
β	Subpopulation diversity contribution threshold	0.32
λ	Population contribution threshold	0.02
θ	Population diversity threshold	0.13

The purpose of the maximum propagation metric is to calculate the Euclidean distance between the extreme individuals of the nondominated solution set. The larger the value, the wider the range of Pareto solution sets. It can be calculated by (17).

$$D = \sqrt{\sum_{m=1}^{M} \left(\max_{i=1}^{|P|} f_m^i - \min_{i=1}^{|P|} f_m^i\right)^2}, \quad (17)$$

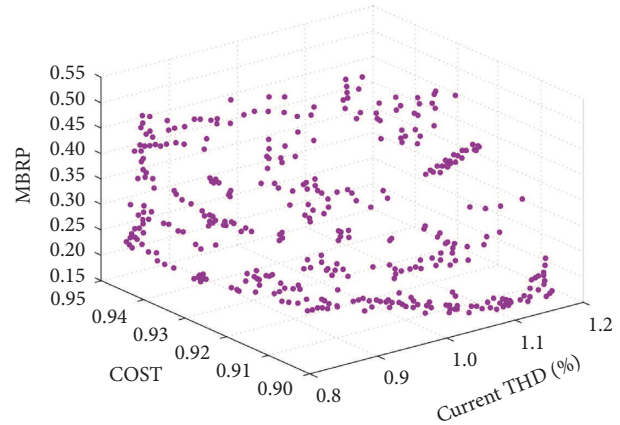

Figure 8: AMP NSGA-II Pareto front solution set.

where M is the number of objective functions and f_m^i is the value of the i-th individual on the objective function m. The results on the two metrics of AMP NSGA-II and conventional NSGA-II are shown in Table 4. It can be seen that the

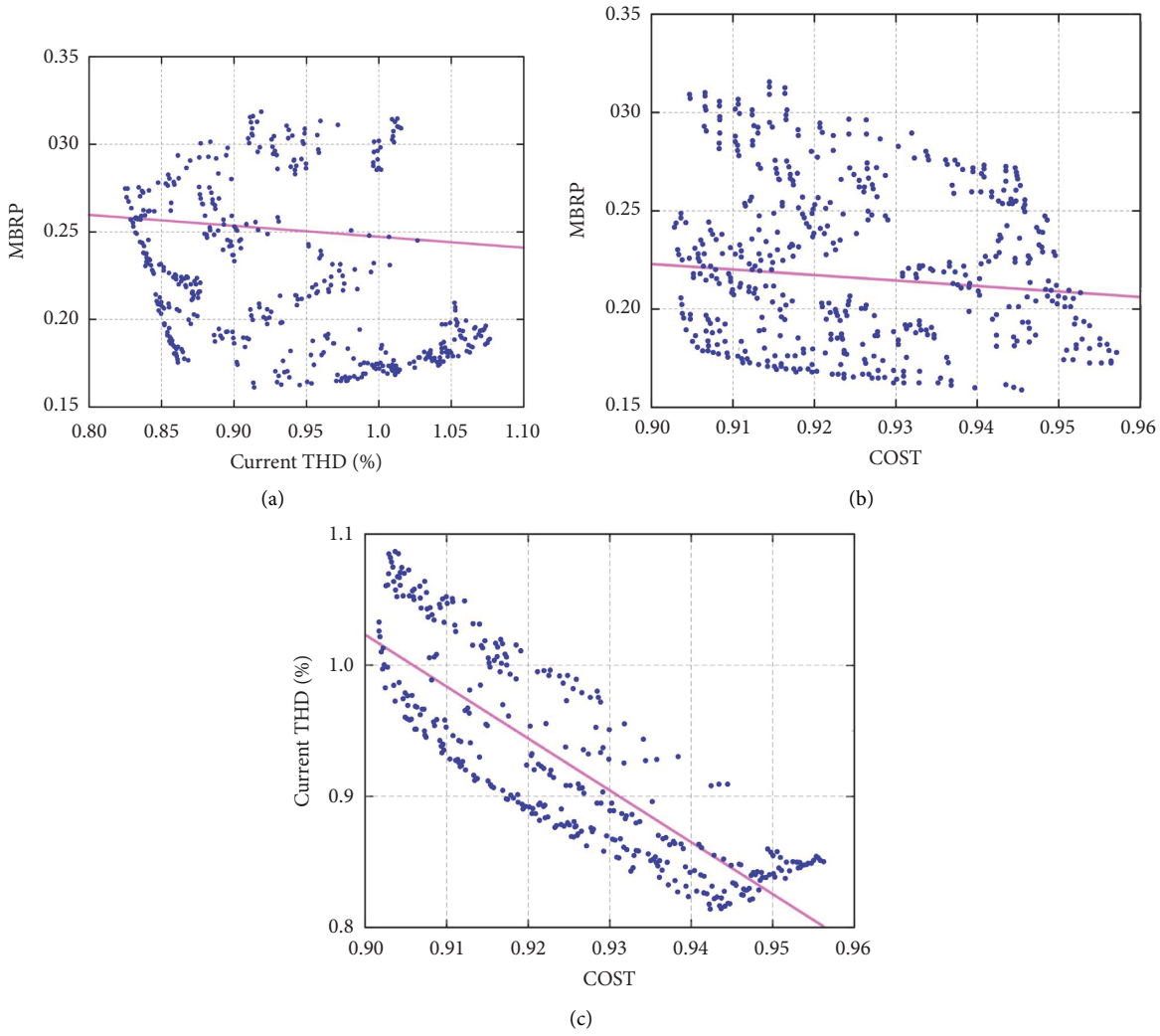

Figure 9: Relationship between the two. (a) MBRP in relation to Current THD%. (b) MBRP in relation to COST. (c) Current THD% in relation to COST.

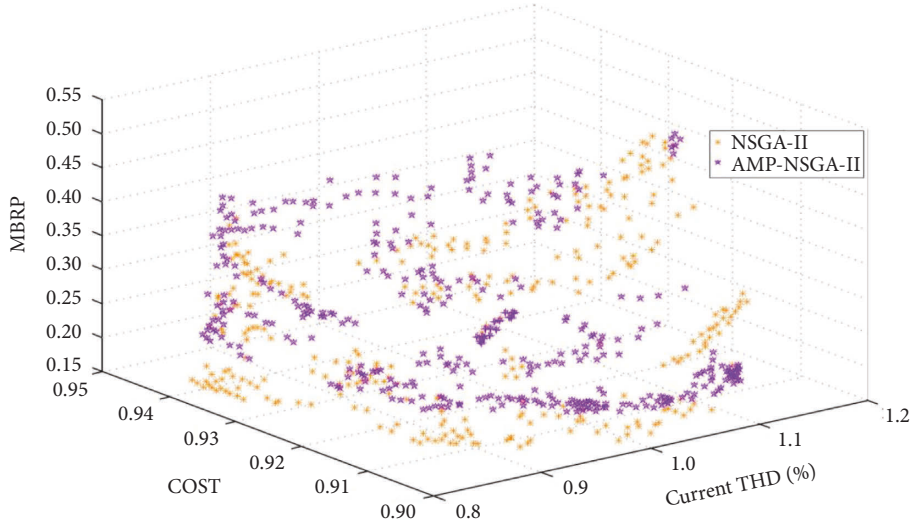

Figure 10: The set of Pareto front solutions for both algorithms.

Table 4: Comparison of algorithm metrics.

Metrics	Median (GD)	Maximum spread
AMP NSGA-II	$1.082e-05$	1.59
NSGA-II	$4.32e-04$	0.82

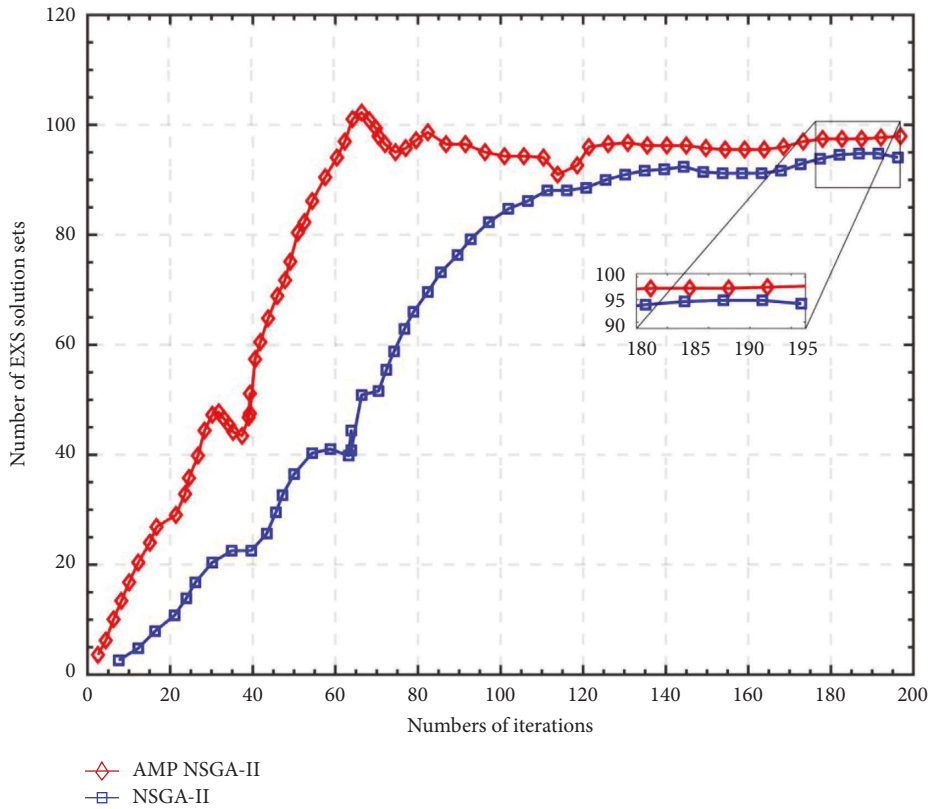

Figure 11: Number of AMP NSGA-II and NSGA-II into EXS solution sets.

solution set of AMP NSGA-II is more uniform and closer to the optimal solution.

Figure 11 then indicates the number of iterations into the EXS solution set when the same number of iterations occur when the two algorithms are performed simultaneously. At the beginning iterations, the AMP NSGA-II algorithm is always more rapid than the traditional NSGA-II, and the rapidity of the AMP NSGA-II algorithm can be illustrated by the fact that when reaching the final stabilization, AMP NSGA-II takes only 120 iterations, while NSGA-II requires 140 iterations. At the end of the iteration, there are also fewer solution sets in traditional NSGA-II than in AMP NSGA-II.

In literature [28] and literature [29], the author was working on a passive filter optimization algorithm, in which he compares the results of the algorithm proposed in the study with some classical algorithms (MOPSO, MOBA, SA) after processing. The GD results show the superiority of the proposed method by showing higher accuracy. Literature [34] also compares these classical algorithms by GD aspects more than SA and MOBA. This study uses AMP-NSGA-II, which can reflect the relevance and conflict of the objective function, i.e., the connection between specific objectives, through the algorithm within the time limit, which is confirmed by the experimental results, which is the biggest innovation of this study, Not only by GD comparison but also by maximum propagation, reflecting the diversity of the multipropagation method. The article is accompanied by a plot of the number of entries into the EXS solution and the number of iterations for the same parameter settings for the proposed method and the most recent study. From Figure 12, it is clear that the proposed method is the smoothest and gets to the steady state the quickest.

In order to demonstrate the efficiency of the proposed method in calculating costs, the proposed method was compared with the latest studies (TLBO, MOBSO, and MOABC) to produce calculation times based on an average of 30 independent operations with the same parameter settings, and the results are included in the table to demonstrate the efficiency of the proposed method. The calculation times for each algorithm are shown in Table 5 for easy comparison.

According to equation (10), the standard deviation of the three objectives can be calculated, and the correlation coefficient matrix can be calculated by equation (11), and then,

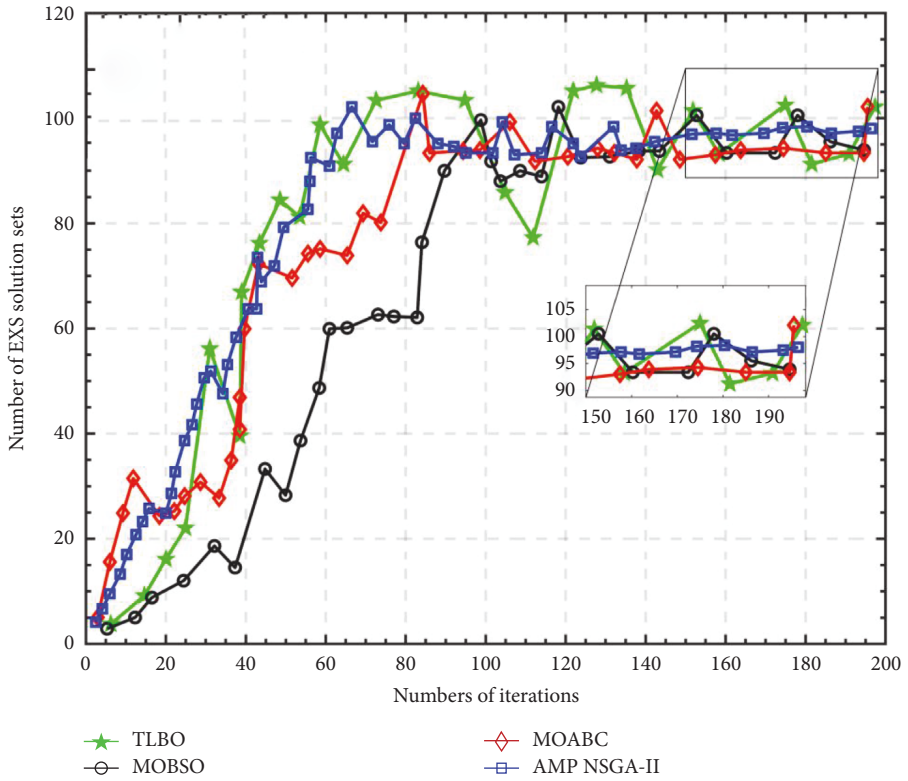

Figure 12: Number of AMP NSGA-II, TLBO, MOBSO, and MOABC into the EXS solution sets.

Table 5: Computational times of the algorithms.

Algorithms	Computational time (s)
AMP NSGA-II	552.65
TLBO [34]	599.18
MOBSO [28]	587.28
MOABC [29]	586.69

according to the standard deviation and correlation coefficient, the weight vectors of the objective function (MBRP, Current THD%, COST) can be calculated as 0.156, 0.386, and 0.458, respectively. The calculation results do not consider the artificial factors, and the results are in line with expected, because companies pay more attention to economic costs.

The results obtained with the proposed optimization algorithm are compared with the results determined by NSGA-II. The hysteresis factor of case III is 0.98, and the units of capacitance (C), inductance (L), and resistance (R) are uf, mH, and Ω. Table 6 shows that the current harmonic distortion rate, overall cost and maintenance cost, and basic reactive power loss ratio results of AMP NSGA-II are smaller than those determined by NSGA-II, and the values are within the IEEE standard range. It can be proved that the parameter performance of AMP NSGA-II is stronger than that of conventional NSGA-II.

The top 10 solutions that will be configured for optimization are shown in Table 7. From the data in the table, it can be seen that the three objectives are not optimal at the same time because there are conflicts and contradictions between them, but in fact, it can be seen that the difference is not very big because the framework is more stable and has good smoothness. The top ranking is the optimal configuration with Current THD% of 0.823, COST of 0.902, and MBRP of 0.232.

Table 6: Comparison of parameters under two algorithms.

Design projects and target value	AMP NSGA-II	NSGA-II
Compensation capacitor	C_4 = 3.4648	C_4 = 3.4523
C-type filter	C_1 = 68.31	C_1 = 65.20
	C_2 = 5.2544	C_2 = 5.0123
	R_1 = 434.26	R_1 = 433.96
	L_1 = 148.32	L_1 = 147.22
	C_3 = 5.2544	C_3 = 5.1232
Second-order high-pass filter	R_2 = 110.1405	R_2 = 110.1254
	L_2 = 15.936	L_2 = 15.565
Current THD%	0.823	0.884
COST	0.902	0.934
MBRP	0.232	0.375

Table 7: Specific parameters of the first 10 optimal solutions.

Subserial number	Design variables								Objectives		
	C_1	C_2	C_3	C_4	R_1	R_2	L_1	L_2	COST	MBRP	Current THD%
1	68.31	5.2544	5.2544	3.4648	434.3	110.1405	148.32	15.936	0.902	0.232	0.823
2	68.32	5.2655	5.2655	3.4655	434.0	110.1421	148.33	15.925	0.911	0.235	0.819
3	68.30	5.2543	5.2544	3.4645	434.6	110.1652	148.20	15.933	0.914	0.234	0.822
4	68.32	5.2631	5.2632	3.5100	434.3	110.1505	148.62	15.933	0.915	0.232	0.836
5	68.33	5.2546	5.2544	3.4544	434.2	110.1409	148.23	15.922	0.915	0.246	0.833
6	68.29	5.2546	5.2548	3.4556	434.2	110.1526	148.31	15.945	0.924	0.235	0.835
7	68.31	5.2655	5.2652.	3.4645	434.3	110.1512	148.33	15.663	0.926	0.262	0.854
8	68.33	5.2544	5.2435	3.4648	434.2	110.1408	148.36	15.906	0.901	0.256	0.856
9	68.31	5.2633	5.2630	3.4625	434.6	110.1418	148.29	15.962	0.923	0.315	0.882
10	68.31	5.2546	5.2648	3.4820	434.3	110.1500	148.30	15.954	0.923	0.337	0.892

6. Conclusions

The optimization of the PPF is a promising option. In this study and in this section, we apply to a two-stage decision framework to determine the design and optimization of PPF. In the first stage, the minimum harmonic current distortion rate (Current THD%), the overall cost and maintenance cost (COST), and the minimum basic reactive power loss (MBRP) are coded as objective functions and designed as multiobjective optimization models. Then, the AMP NSGA-II algorithm with multiple group multiple crossover operations is used, and the logistic model is adaptively adjusted to derive the Pareto front in the EXS solution set. In the second stage, the weights of the objective function are determined using the criterion importance interrelationship (CRITIC), and the unique optimal solution is selected using the similarity ranking preference technique (TOPSIS). After a two-stage decision framework, an optimal solution is obtained with an optimal configuration of Current THD% of 0.823, COST of 0.902, and MBRP of 0.232. (1) In the study, the results are compared with the traditional classical NSGA-II, and the high performance of AMP NSGA-II is demonstrated using GD with maximum propagation. (2) Based on the number of iterations with the EXS solution set, the superiority and rapidity of the optimization algorithm are demonstrated based on the number of iterations and the number of solutions in the EXS solution set. (3) Based on the CRITIC-TOPSIS method, it is concluded that the COST weight is the largest and meets the actual requirements of the enterprise. (4) Based on the Pareto front scheme, it is concluded that the traditional NSGA-II distribution solution is inferior to AMP NSGA-II, proving the existence of contradictory conflicts in the three objectives. (5) The two-stage framework in the study can help decision makers to solve multiobjective optimization problems easily and clearly, creating a PPF design solution in the context of extra-high voltage. In summary, the two-stage framework in the study covers the advanced AMP NSGA-II algorithm, which is perfectly matched with the CRITIC-TOPSIS decision, and will not only have a good performance in filters but also have a better prospect in solving other multi-objective optimization problems, and it is worth promoting and studying in depth.

In future work for practical problems in UHVDC system, it is important to take into account dynamic balancing problems, i.e., when encountering parameter variations, such as errors in the rectifier-side impedance or deviations in the trigger angle, which are not taken into account in the proposed algorithm. Furthermore, this topic can be extended to the optimization and control applications of battery systems for electric vehicles [55].

Data Availability

The data used to support the findings of this study are available from the corresponding author upon request.

Conflicts of Interest

The authors declare that they have no conflicts of interest regarding the publication of this study.

Acknowledgments

The study was supported by the Jilin Provincial Development and Reform Commission (Grant: 2018C035-1), the Jilin Provincial Development and Reform Commission (Grant: 2022C045-11), the Project of Science and Technology Department of Jilin Province: High-Power Electronic Technology and Parallel Robot Technology Innovation Team of Jilin Province (20190101018JH).

References

[1] L. Leite, W. Boaventura, L. Errico, E. Cardoso, R. Dutra, and B. Lopes, "Integrated voltage regulation in distribution grids with photovoltaic distribution generation assisted by telecommunication infrastructure," *Electric Power Systems Research*, vol. 136, pp. 110–124, 2016.

[2] I. Y. Chung, "Development of power quality diagnosis system for power quality improvement," in *Proceedings of the 2003 Ieee Power Engineering Society General Meeting*, vol. 1-4, pp. 1256–1261, New York, 2003.

[3] S. R. Gampa and D. Das, "Optimum placement of shunt capacitors in a radial distribution system for substation power factor improvement using fuzzy GA method," *International Journal of Electrical Power & Energy Systems*, vol. 77, pp. 314–326, May 2016.

[4] I. Diaaeldin, S. Abdel Aleem, A. El-Rafei, A. Abdelaziz, and A. F. Zobaa, "Optimal network reconfiguration in active distribution networks with soft open points and distributed generation," *Energies*, vol. 12, no. 21, p. 4172, 2019.

[5] L. Michalec, M. Jasinski, T. Sikorski, Z. Leonowicz, L. Jasinski, and V. Suresh, "Impact of harmonic currents of nonlinear loads on power quality of a low voltage network-review and case study," *Energies*, vol. 14, no. 12, p. 3665, 2021.

[6] I. Wallace, "Harmonic mitigation strategies in variable frequency drive applications," *ASHRAE Transactions*, vol. 127, pp. 452–459, 2021, https://www.webofscience.com/wos/woscc/full-record/WOS:000725205700052.

[7] S. Golestan, J. M. Guerrero, J. C. Vasquez, A. M. Abusorrah, and Y. Al-Turki, "Harmonic linearization and investigation of three-phase parallel-structured signal decomposition algorithms in grid-connected applications," *IEEE Transactions on Power Electronics*, vol. 36, no. 4, pp. 4198–4213, 2021.

[8] A. Manito, U. Bezerra, M. Tostes, E. Matos, C. Carvalho, and T. Soares, "Evaluating harmonic distortions on grid voltages due to multiple nonlinear loads using artificial neural networks," *Energies*, vol. 11, no. 12, p. 3303, 2018.

[9] J. Kwon, X. Wang, F. Blaabjerg, and C. L. Bak, "Frequency-domain modeling and simulation of dc power electronic systems using harmonic state space method," *IEEE Transactions on Power Electronics*, vol. 32, no. 2, pp. 1044–1055, 2017.

[10] M. Tumay, T. Demirdelen, S. Bal, R. I. Kayaalp, B. Dogru, and M. Aksoy, "A review of magnetically controlled shunt reactor for power quality improvement with renewable energy applications," *Renewable and Sustainable Energy Reviews*, vol. 77, pp. 215–228, 2017.

[11] L. Ding, Q.-L. Han, B. Ning, and D. Yue, "Distributed resilient finite-time secondary control for heterogeneous battery energy storage systems under denial-of-service attacks," *IEEE Transactions on Industrial Informatics*, vol. 16, no. 7, pp. 4909–4919, 2020.

[12] Q.-V. Pham, F. Fang, V. N. Ha et al., "A survey of multi-access edge computing in 5g and beyond: fundamentals, technology integration, and state-of-the-art," *IEEE Access*, vol. 8, pp. 116974–117017, 2020.

[13] S. M. Ismael, S. H. E. A. Aleem, A. Y. Abdelaziz, and A. F. Zobaa, "State-of-the-art of hosting capacity in modern power systems with distributed generation," *Renewable Energy*, vol. 130, pp. 1002–1020, 2019.

[14] M. Zhang and H. Sun, "Improvement of an SVC using an active power filter connected in parallel with synchronous switched capacitors," in *Proceedings of the Iciea 2007: 2nd Ieee Conference on Industrial Electronics and Applications*, vol. 1-4, pp. 212–216, 2007, https://www.webofscience.com/wos/woscc/full-record/WOS:000252231900044.

[15] D. Li, K. Yang, Z. Q. Zhu, and Y. Qin, "A novel series power quality controller with reduced passive power filter," *IEEE Transactions on Industrial Electronics*, vol. 64, no. 1, pp. 773–784, 2017.

[16] M. Jayaraman and S. Vt, "Power quality improvement in a cascaded multilevel inverter interfaced grid connected system using a modified inductive-capacitive-inductive filter with reduced power loss and improved harmonic attenuation," *Energies*, vol. 10, no. 11, p. 1834, 2017.

[17] I. Khan, A. S. Vijay, and S. Doolla, "Nonlinear load harmonic mitigation strategies in microgrids: state of the art," *IEEE Systems Journal*, vol. 16, no. 3, pp. 4243–4255, 2022.

[18] A. Menti, T. Zacharias, and J. Milias-Argitis, "Optimal sizing and limitations of passive filters in the presence of background harmonic distortion," *Electrical Engineering*, vol. 91, no. 2, pp. 89–100, 2009.

[19] J. Yang, X. Zhang, K. Zhang, X. Cui, C. Jiao, and X. Yang, "An LCC-SP compensated inductive power transfer system and design considerations for enhancing misalignment tolerance," *IEEE Access*, vol. 8, pp. 193285–193296, 2020.

[20] S. H. Abdel Aleem, A. F. Zobaa, and M. E. Balci, "Optimal resonance-free third-order high-pass filters based on minimization of the total cost of the filters using Crow Search Algorithm," *Electric Power Systems Research*, vol. 151, pp. 381–394, 2017.

[21] A. Bagheri and M. Alizadeh, "Designing a passive filter for reducing harmonic distortion in the hybrid micro-grid including wind turbine, solar cell and nonlinear load," *Przeglad Elektrotechniczny*, vol. 1, no. 12, pp. 11–14, 2019.

[22] C. Gurrola-Corral, J. Segundo, M. Esparza, and R. Cruz, "Optimal LCL-filter design method for grid-connected renewable energy sources," *International Journal of Electrical Power & Energy Systems*, vol. 120, p. 105998, 2020.

[23] S. Shakeri, S. Esmaeili, and M. H. Rezaeian, "Passive harmonic filter design considering voltage sag performance-applicable to large industries," *IEEE Transactions on Power Delivery*, vol. 37, no. 3, pp. 1714–1722, 2022.

[24] Y.-J. Kim and H. Kim, "Optimal design of LCL filter in grid-connected inverters," *IET Power Electronics*, vol. 12, no. 7, pp. 1774–1782, 2019.

[25] Y. Terriche, D. Kerdoun, S. Golestan, A. Laib, H. Djehloud, and J. M. Guerrero, "Effective and low-cost passive compensator system to improve the power quality of two electric generators," *IET Power Electronics*, vol. 12, no. 7, pp. 1833–1840, 2019.

[26] R. Klempka, "Optimal double-tuned filter efficiency analysis," *IEEE Transactions on Power Delivery*, vol. 36, no. 2, pp. 1079–1088, 2021.

[27] D. Solatialkaran, K. G. Khajeh, and F. Zare, "A novel filter design method for grid-tied inverters," *IEEE Transactions on Power Electronics*, vol. 36, no. 5, pp. 5473–5485, 2021.

[28] N.-C. Yang and D. Mehmood, "Multi-objective bee swarm optimization algorithm with minimum manhattan distance for passive power filter optimization problems," *Mathematics*, vol. 10, no. 1, p. 133, 2022.

[29] N.-C. Yang, D. Mehmood, and K.-Y. Lai, "Multi-objective artificial bee colony algorithm with minimum manhattan distance for passive power filter optimization problems," *Mathematics*, vol. 9, no. 24, p. 3187, 2021.

[30] J. Khajouei, S. Esmaeili, and S. M. Nosratabadi, "Optimal design of passive filters considering the effect of Steinmetz circuit resonance under unbalanced and non-sinusoidal conditions," *IET Generation, Transmission & Distribution*, vol. 14, no. 12, pp. 2333–2344, Jun, 2020.

[31] M. Bajaj, N. K. Sharma, M. Pushkarna, H. Malik, M. A. Alotaibi, and A. Almutairi, "Optimal design of passive power filter using multi-objective pareto-based firefly algorithm and analysis under background and load-side's nonlinearity," *IEEE Access*, vol. 9, pp. 22724–22744, 2021.

[32] T. A. H. Alghamdi, F. Anayi, and M. Packianather, "Optimal design of passive power filters using the mrfo algorithm and a practical harmonic analysis approach including uncertainties in distribution networks," *Energies*, vol. 15, no. 7, p. 2566, 2022.

[33] M. Ayoubi and R.-A. Hooshmand, "A new fuzzy optimal allocation of detuned passive filters based on a Nonhomogeneous Cuckoo Search Algorithm considering resonance constraint," *ISA Transactions*, vol. 89, pp. 186–197, 2019.

[34] N.-C. Yang and S.-W. Liu, "Multi-objective teaching-learning-based optimization with pareto front for optimal design of passive power filters," *Energies*, vol. 14, no. 19, p. 6408, 2021.

[35] N. M. Khattab, S. H. Abdel Aleem, A. El'Gharably et al., "A novel design of fourth-order harmonic passive filters for total demand distortion minimization using crow spiral-based search algorithm," *Ain Shams Engineering Journal*, vol. 13, no. 3, Article ID 101632, 2022.

[36] M. Bajaj and A. K. Singh, "Optimal design of passive power filter for enhancing the harmonic-constrained hosting capacity of renewable DG systems," *Computers & Electrical Engineering*, vol. 97, p. 107646, 2022.

[37] M. H. Arshad, M. A. Abido, A. Salem, and A. H. Elsayed, "Weighting factors optimization of model predictive torque control of induction motor using NSGA-II with TOPSIS decision making," *IEEE Access*, vol. 7, pp. 177595–177606, 2019.

[38] L. Xiaoqing, D. Haiying, L. Hongwei, L. Mingxue, and S. Zhiqiang, "Optimization control of front-end speed regulation (FESR) wind turbine based on improved NSGA-II," *IEEE Access*, vol. 7, pp. 45583–45593, 2019.

[39] B. Wang, H. Xie, X. Xia, and X. Zhang, "A NSGA-II algorithm hybridizing local simulated-annealing operators for a Bi-criteria robust job-shop scheduling problem under scenarios," *IEEE Transactions on Fuzzy Systems*, vol. 27, no. 5, pp. 1075–1084, 2019.

[40] M. E. Hamidi and R. M. Chabanloo, "Optimal allocation of distributed generation with optimal sizing of fault current limiter to reduce the impact on distribution networks using NSGA-II," *IEEE Systems Journal*, vol. 13, no. 2, pp. 1714–1724, 2019.

[41] N. K. Kamila, L. Jena, and H. K. Bhuyan, "Pareto-based multi-objective optimization for classification in data mining," *Cluster Computing*, vol. 19, no. 4, pp. 1723–1745, 2016.

[42] G. Yildirim and B. Alatas, "New adaptive intelligent grey wolf optimizer based multi-objective quantitative classification rules mining approaches," *Journal of Ambient Intelligence and Humanized Computing*, vol. 12, no. 10, pp. 9611–9635, 2021.

[43] S. Qiao, X. Dai, Z. Liu, J. Huang, and G. Zhu, "Improving the optimization performance of NSGA-II algorithm by experiment design methods," in *Proceedings of the 2012 IEEE International Conference on Computational Intelligence for Measurement Systems and Applications (CIMSA) Proceedings*, pp. 82–85, July 2012.

[44] S. Yijie and S. Gongzhang, "Improved NSGA-II multi-objective genetic algorithm based on hybridization-encouraged mechanism," *Chinese Journal of Aeronautics*, vol. 21, no. 6, pp. 540–549, 2008.

[45] M. H. Shojaeefard, S. E. Hosseini, and J. Zare, "CFD simulation and Pareto-based multi-objective shape optimization of the centrifugal pump inducer applying GMDH neural network, modified NSGA-II, and TOPSIS," *Structural and Multidisciplinary Optimization*, vol. 60, no. 4, pp. 1509–1525, 2019.

[46] W. Yang and Y. Pang, "New q-Rung orthopair hesitant fuzzy decision making based on linear programming and TOPSIS," *IEEE Access*, vol. 8, pp. 221299–221311, 2020.

[47] T. Samala, V. K. Manupati, J. Machado, S. Khandelwal, and K. Antosz, "A systematic simulation-based multi-criteria decision-making approach for the evaluation of semi-fully flexible machine system process parameters," *Electronics*, vol. 11, no. 2, p. 233, 2022.

[48] F. Xu, J. Liu, S. Lin, Q. Dai, and C. Li, "A multi-objective optimization model of hybrid energy storage system for non-grid-connected wind power: a case study in China," *Energy*, vol. 163, pp. 585–603, 2018.

[49] Y. Luo, J. Hu, M. Song, and D. Li, "Simplified design of passive filters for series hybrid active power filters," *Power Grid Technology*, vol. 42, no. 4, pp. 1149–1156, 2018.

[50] M. Zhang and Y. Li, "Multi-objective optimal reactive power dispatch of power systems by combining classification-based multi-objective evolutionary algorithm and integrated decision making," *IEEE Access*, vol. 8, pp. 38198–38209, 2020.

[51] Y. Li, J. Wang, D. Zhao, G. Li, and C. Chen, "A two-stage approach for combined heat and power economic emission dispatch: combining multi-objective optimization with integrated decision making," *Energy*, vol. 162, pp. 237–254, 2018.

[52] X. Xu, W. Hu, D. Cao, Q. Huang, C. Chen, and Z. Chen, "Optimized sizing of a standalone PV-wind-hydropower station with pumped-storage installation hybrid energy system," *Renewable Energy*, vol. 147, pp. 1418–1431, 2020.

[53] D. Diakoulaki, G. Mavrotas, and L. Papayannakis, "Determining objective weights in multiple criteria problems: the critic method," *Computers & Operations Research*, vol. 22, no. 7, pp. 763–770, 1995.

[54] N. A. Azhar, N. A. M. Radzi, and W. S. H. M. W. Ahmad, "Multi-criteria decision making: a systematic review," *Recent. Adv. Electr. Electron. Eng.*vol. 14, no. 8, pp. 779–801, 2021.

[55] K. Li, H. Wang, C. Xu et al., "Multi-objective optimization of side plates in a large format battery module to mitigate thermal runaway propagation," *International Journal of Heat and Mass Transfer*, vol. 186, Article ID 122395, 2022.